Supporting Information

A single-molecular ruthenium(II) complex-based NIR-II fluorophore for enhanced chemo-photothermal therapy

Qianqian Li [ab, †], Yishen Liu [a †], Bingshan Zhao [b †], Jiapeng Lei [c †], Siyu Lu [a], Wanxia Gong [a], Ke Liang [a], Junzhu Wu [d], Xuechuan Hong *[ad] and Yuling Xiao*[a]

a. Department of Cardiology, Zhongnan Hospital of Wuhan University, School of Pharmaceutical Sciences, Wuhan University, Wuhan 430071, China. E-mail: xiaoyl@whu.edu.cn.

b. Hubei Key Laboratory for Processing and Application of Catalytic Materials, Huanggang Normal University, Huanggang, 438000, China

c. School of Basic Medical Sciences, Nanchang University, Nanchang, 330031, P.R. China

d. State Key Laboratory of Virology, Key Laboratory of Combinatorial Biosynthesis and Drug Discovery (MOE), Hubei Provincial Key Laboratory of Developmentally Originated Disease, Center for Experimental Basic Medical Education, Wuhan 430071, China

† These authors contributed equally to this work.

Author contributions

X. Hong and Y. Xiao designed the research; Q. Li, Y. Liu, B. Zhao, and J. Lei synthesized NIR-II fluorophores; Q. Li, Y. Liu, B. Zhao, S. Lu, W. Gong, K. Liang and J. Wu conducted the in vitro and in vivo studies; Q. Li, Y. Liu, X. Hong and Y. Xiao analyzed data and wrote the paper.

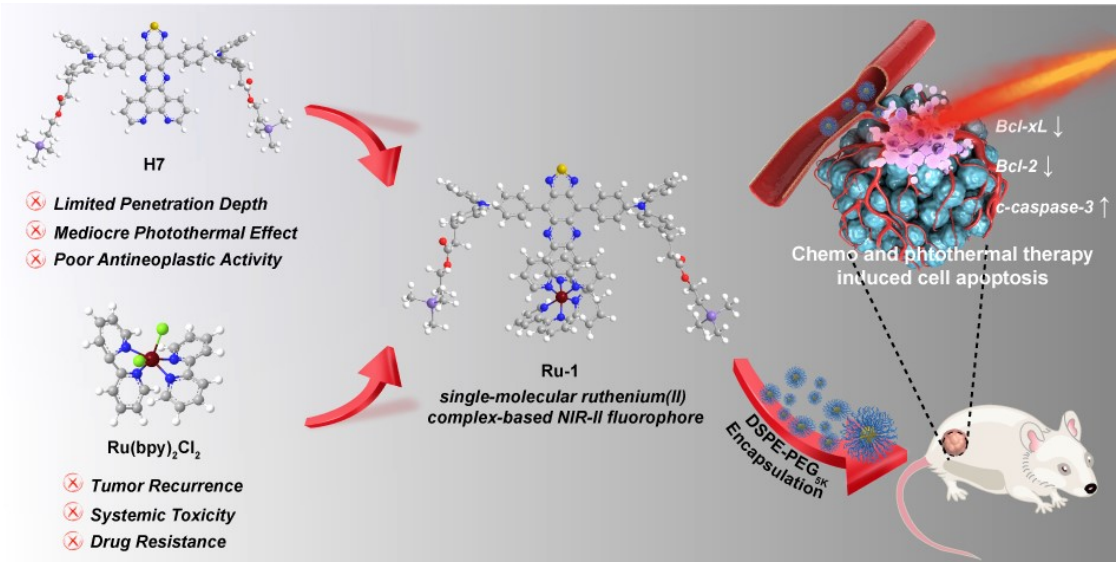

A novel NIR-II Ru(II) polypyridyl fluorophore Ru-1 dots was designed and synthesized for synergistic chemo-photothermal therapy against 4T1 tumors through cell apoptosis pathway

Materials and General Procedure

The chemical reagents were purchased from commercial suppliers (such as Aldrich, Adamas, Energy Chemical, Sinopharm Group Co., Ltd.) and used without further purification unless otherwise noted. Tetrahydrofuran (THF) was freshly distilled from sodium/benzophenone. Dimethylformamide (DMF) and dichloromethane (CH_2Cl_2) were distilled from calcium hydride. Anhydrous pyridine was freshly distilled using calcium hydride. Intermediate-**1** was synthesized according to our previous report.[1] ^1H and ^{13}C NMR spectra were recorded in $CDCl_3$ and *d*6-DMSO at room temperature using a Bruker AV400 magnetic resonance spectrometer. ESI-MS were performed on Finnigan LCQ advantage mass spectrometer. MALDI-TOF-MS characteristics were performed on an AB SCIEX 5800 MALDI TOF mass spectrometer. Analytical and preparative TLC were performed on silica gel plates, and column chromatography was conducted over silica gel (mesh 200-300), both of which were obtained from the Qingdao Ocean Chemicals. UV-vis-NIR spectra were tested with a SHIMADZU UV-2600 or PerkinElmer Lambda 25 spectrophotometer. NIR fluorescence spectrum was performed on an Applied Nano Fluorescence spectrometer at room temperature with an excitation laser source of 785 nm. The NIR-II *in vivo* imaging system was purchased from Suzhou NIR-Optics Technologies CO., Ltd.

Synthesis and characterization

1. Synthetic procedures of intermediate-1

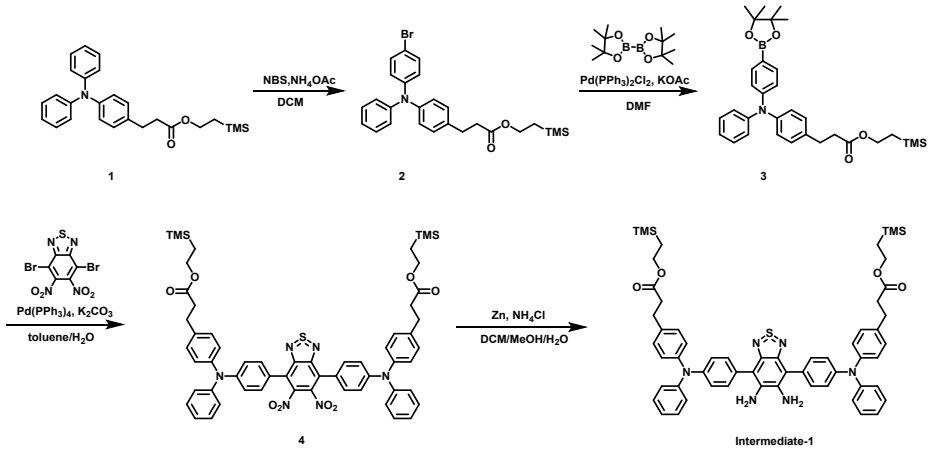

The intermediate-**1** was obtained from compound **1** according to our previous report.[1]

2. Synthetic procedures of Ru-1 and H7

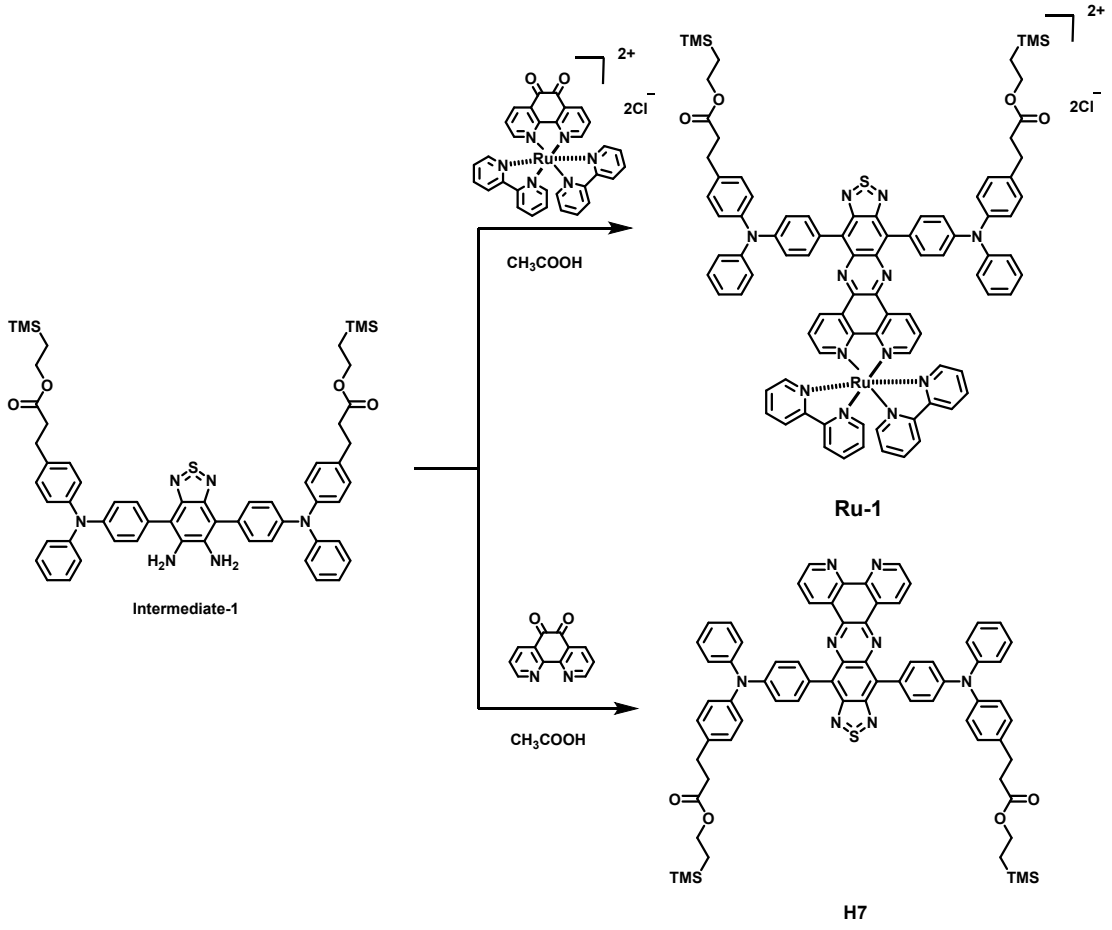

Synthesis of compound **H7**

To a solution of intermediate-**1** (80 mg, 0.076 mmol) in acetic acid (5 mL) was added 1,10-phenanthroline-5,6-dione (20 mg, 0.09 mmol). The resulting mixture was heated to reflux under N_2

atmosphere. After reaction was complete, the mixture was concentrated to give a residue, the residue was further purified by column chromatography to give **H7** as a green solid (35 mg, yield 39.33%). ^{1}H NMR (400 MHz, $CDCl_3$) δ 9.23-9.21 (m, 4H), 8.00 (d, *J* = 8.4 Hz, 4H), 7.70 (dd, *J* = 7.7, 4.6 Hz, 2H), 7.39–7.29 (m, 12H), 7.28-7.25 (m, 4H) ,7.21-7.19 (m, 4H), 7.12 (t, *J* = 6.8 Hz, 2H), 4.20 (t, *J* = 7.8 Hz, 4H), 2.97 (t, *J* = 7.8 Hz, 4H), 2.65 (t, *J* = 7.8 Hz, 4H), 0.99 (t, *J* = 7.8 Hz, 4H), 0.04 (s, 18H). ^{13}C NMR (101 MHz, $CDCl_3$) δ 173.1, 153.0, 152.9, 149.4, 148.3, 147.5, 145.6, 142.1, 137.3, 136.2, 134.4, 134.1, 129.4, 129.4, 129.2, 128.1, 127.9, 125.6, 125.2, 124.6, 123.6, 121.1, 62.8, 36.1, 30.5, 17.3, 1.44. MALDI-TOF-MS m/z: $[M+H]^+$ calcd for $C_{70}H_{67}N_8O_4SSi_2$, 1172.599; found, 1173.1.

Synthesis of compound **Ru(bpy)$_2$(phendione)Cl$_2$**

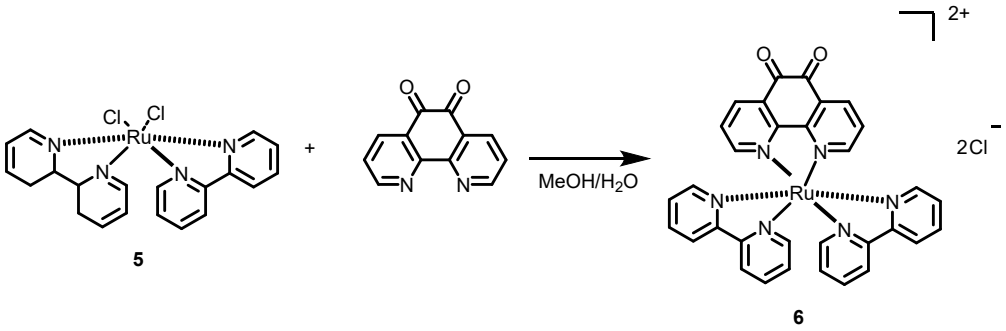

To a solution of compound **5** (61 mg, 0.125 mmol) in MeOH (2 mL) and H_2O (2 mL) was added 1,10-phenanthroline-5,6-dione (26.47 mg, 0.125 mmol). The resulting mixture was heated to 90 °C for 8 h. The reaction was monitored by TLC. After reaction was complete, the mixture was cooled to room temperature and added acetone (20 mL) for precipitation at 0 °C for overnight. Then the above mixture was filtered and the filter cake was washed with cold water and recrystallized in diethyl ether (20 mL) to afford compound **6 Ru(bpy)$_2$(phendione)Cl$_2$** as a black solid (50 mg, yield 54%). ^{1}H NMR (400 MHz, DMSO-*d6*) δ 8.95 (d, *J* = 7.0 Hz, 4H), 8.53 (d, *J* = 7.5 Hz, 2H), 8.21 (d, *J* = 3.2 Hz, 4H), 7.96 (d, *J* = 4.7 Hz, 2H), 7.81 (d, *J* = 5.0 Hz, 2H), 7.73 (dd, *J* = 12.7, 6.2 Hz, 4H), 7.59 (d, *J* = 5.7 Hz, 4H). ^{13}C NMR (101 MHz, *d6*-DMSO) δ 174.0, 157.1, 157.0, 156.2, 154.8, 152.2, 151.8, 138.7, 138.6, 135.1, 123.5, 129.0, 128.4, 128.2, 125.2, 125.1.

Synthesis of compound **Ru-1**

To a solution of intermediate-**1** (35 mg, 0.033 mmol) in acetic acid (5 mL) was added

$Ru(bpy)_2(phendione)Cl_2$ (23 mg, 0.033 mmol). The resulting mixture was heated to reflux under N_2 atmosphere. After reaction was complete, the mixture was concentrated to give a residue, the residue was further purified by column chromatography to give **Ru-1** as a yellow-green solid. (15 mg, yield 33%). ^{1}H NMR (400 MHz, $CDCl_3$) δ 9.31 (d, *J* = 8.0 Hz, 2H), 8.96 (t, *J* = 9.0 Hz, 4H), 8.31 (d, *J* = 4.9 Hz, 2H), 8.17 (t, *J* = 7.7 Hz, 2H), 8.09 (t, *J* = 7.7 Hz, 2H), 7.98 (dd, *J* = 16.3, 6.8 Hz, 10H), 7.67–7.60 (m, 2H), 7.53–7.46 (m, 2H), 7.38–7.28 (m, 11H), 7.22 (dd, *J* = 21.5, 8.3 Hz, 8H), 7.12 (t, *J* = 6.8 Hz, 3H), 4.28–4.11 (m, 4H), 2.96 (t, *J* = 7.7 Hz, 4H), 2.64 (t, *J* = 7.7 Hz, 4H), 1.13–0.90 (m, 4H), 0.05 (s, 18H). ^{13}C NMR (101 MHz, $CDCl_3$) δ 173.1, 156.8, 154.0, 153.5, 151.8,151.6,151.0,148.7, 147.2, 145.3, 139.9, 138.7, 138.6,137.2, 136.4, 134.3, 134.1, 131.1, 130.0, 129.5, 129.4, 128.4, 127.4, 125.8, 125.5, 123.9, 120.7, 62.7, 36.1, 30.4, 17.3, 1.4. MALDI-TOF-MS *m*/*z*: $[M\text{-}2Cl]^{2+}$ calcd for $C_{90}H_{82}N_{12}O_4RuSSi_2^{2+}$,1584.49; found,1584.1189.

Cell Culture and Animal Model

Mouse breast cancer cells 4T1 were purchased from the China Center for Type Culture Collection (CCTCC). All cells were grown in a humidified atmosphere at 37 °C with 5% CO_2 atmosphere. 4T1 cells were maintained in Dulbecco's Modified Eagle Medium (DMEM, Gibco), supplemented with 10% fetal bovine serum, 100 IU mL^{-1} penicillin, 100 μg mL^{-1} streptomycin. For 4T1 subcutaneous tumor model establishment, 4T1 cells (roughly 2×10^6 in 75 μL of FBS-free DMEM medium) were subcutaneous injected into the right back leg of the 6-week-old female Balb/c mice which were purchased from Charles River Laboratories (Beijing, China). The tumors were allowed to reach ~200 mm^3 for small animal fluorescent imaging and ~100 mm^3 for *in vivo* therapeutic studies, respectively. (tumor volume = Length*Width*Width/2). And 6-week-old female ICR mice were purchased for biosafety investigation. All animal experiments were performed according to the Chinese Regulations for the Administration of Affairs Concerning Experimental Animals and approved by the Institutional Animal Care and Use Committee (IACUC) of Wuhan University.

Preparation and Characterization of Ru-1 dots

Ru-1 (5 mg) and DSPE-PEG_{5K} (40 mg) were completely dissolved in THF (1 mL). Then the mixture was added dropwise into one grade water (10 mL) under strong sonication. After 5 min sonication, the organic solvent was removed under N_2 flow, then the resulting mixture was washed several

times using a 30 kDa centrifugal filter units and concentrated to yield **Ru-1** dots (~ 5 mg/mL). The resulting **Ru-1** dots was stored in dark at 4 ^{o}C for further usage. The size and morphology were characterized by Transmission electron microscopy (TEM) images on a JEM-2100 TEM system at an accelerating voltage of 200 kV. The hydrodynamic diameter and zeta potentials were measured using a Malvern Zetasizer Nano ZS. The UV-vis-NIR spectra of **Ru-1** dots was tested with a PerkinElmer Lambda 25 UV-Vis spectrophotometer. The corresponding NIR fluorescence spectrum was recorded on an Applied Nano Fluorescence spectrometer at room temperature with an excitation laser source of 785 nm.

***In Vitro* Cell Viability Studies：**

Mouse breast cancer cell lines 4T1 and human hepatic cell lines LO2 were seeded into 96-well plates at a density of 5000 cells/well and maintained in DMEM supplemented with 10% FBS at 37 ^{o}C in a humidified atmosphere containing 5% CO_2. After incubating for 12 h, the cell culture medium was replaced with 100 μL of fresh culture medium containing different concentrations of cisplatin and **Ru-1** dots with or without 808 nm laser irradiation (1 W cm^{-2}, 10 min), and the treated cells were incubated for other 24 h and the cell viability was measured with a MTT standard assay.

Calcein-AM/PI staining assay

Cell cultures were washed with PBS and treated with DMEM containing **Ru-1** dots (20 μM) for 24 h in the presence or absence of 808 nm laser irradiation. And the other two cell cultures were treated with DMEM in the presence or absence of laser irradiation for comparsion. Subsequently, the cell cultures in each group were carefully washed with 100 μL PBS and added paraformaldehyde fix solution for cell immobilization. Then living and dead cells staining were conducted by using Calcein-AM/PI Assay Kit (Solarbio, China) according to the manufacturer's instructions and the literature procedure.[2] Finally, cell fluorescence imaging of these cells was conducted to evaluate the anti-tumor activities of **Ru-1** dots through an inverted fluorescence microscope (Olympus ,USA). All samples were repeated more than three times to ensure accuracy.

Flow cytometry assay

4T1 cells were cultured in 6-well plates and then treated with 20 μM **Ru-1** dots for 24 h. After irradiation with or without 808 nm laser (1 W cm^{-2}, 5 min), the cells were resuspended in PBS. The cell samples were processed to evaluate the cell cycle according to the instructions of the Annexin V-FITC/PI apoptosis kit (Multi Sciences, China), and then tested with the FACS Canto II cytometer (Beckman Cytexpert). All samples were repeated more than three times to ensure accuracy.

Western blot assay

The treated 4T1 cells were lysed with radioimmunoassay (RIPA) lysis buffer. SDS-PAGE gel electrophoresis was performed on the equal amount of protein samples according to the BCA method. Through membrane transfer and blocking, and incubated with the following antibodies: cleaved caspase-3 (1: 1000, CST, America), Bcl-2 (1: 2500, proteintech, China), Bcl-xL (1: 2500, proteintech, China), β-actin (1:10000, proteintech, China) and horseradish peroxidase-conjugated secondary antibodies (1: 10000, proteintech, China). Finally, the chemiluminescence imaging system (ChemiDoc XRS+) was used for membrane observation. All samples were repeated more than three times to ensure accuracy.

Photothermal performance measurement

The temperature curve over time was plotted through employing an infrared thermal camera (FORTRIC 225) to record the temperature variation in **Ru-1** dots (200 μL) with different concentration (0 μM, 20 μM, 40 μM, 80 μM, 100 μM) under 808 nm laser irradiation (1 W cm^{-2}, 5 min). The photothermal conversion efficiency (η) of **Ru-1** dots was calculated according to the equation as follows in previous report [2]:

$$\eta = \frac{hS\Delta T_{max} - Q_s}{I(1 - 10^{-A808})}$$

where, h represents the heat transfer coefficient, S is the surface area of the vessel, ΔT_{max} represents the maximum temperature variation between maximum steady-state temperature and ambient temperature of the environment, Q_s represents the heat associated with the light absorbance of water and container which can be ignored, I is laser power density, and A_{808} is the absorbance of **Ru-1** dots at 808 nm. and hS = mc/τ. m refers to the solution mass, c means the specific heat capacity of

water, and τ is obtained from the cooling process and time.

***In vivo* NIR-II fluorescence imaging**

For tumor imaging, 4T1 tumor-bearing mice were mounted on the imaging stage with the prone position beneath the laser. NIR-II fluorescence images were collected using a NIR-II imaging system (Suzhou NIR-Optics Technologies CO., Ltd) under an 808 nm laser irradiation with 90 mW cm^{-2} laser power density.[3]

***In vivo* photothermal imaging:**

The Balb/c 4T1 tumor bearing mice were intravenously injected with **Ru-1** dot (2 mg/kg **Ru**). After 24 h post-injection, the aforementioned mice were anesthesized by intraperitoneal injection of pentobarbital sodium solution (50 mg kg-1). And the tumor of the above mice was irradiated with 808 nm laser (1 W cm^{-2}) for 10 min. and the temperature variation of tumor were recorded with an IR thermal camera under irradiation for 10 min to investigate the photothermal effects of **Ru-1** dots.

***In vivo* biodistribution study**

For studying the biodistribution of **Ru-1** dots in mice, the tumor-bearing mice after intravenous of the **Ru-1** dots were sacrificed to collect the major organs and tumors of the mice at post-injections of 12 h, 24 h and 48 h for NIR II fluorescent imaging. And the biodistribution and metabolism of **Ru-1** dots was analyzed by the average fluorescence intensity of each tissue in different time point.

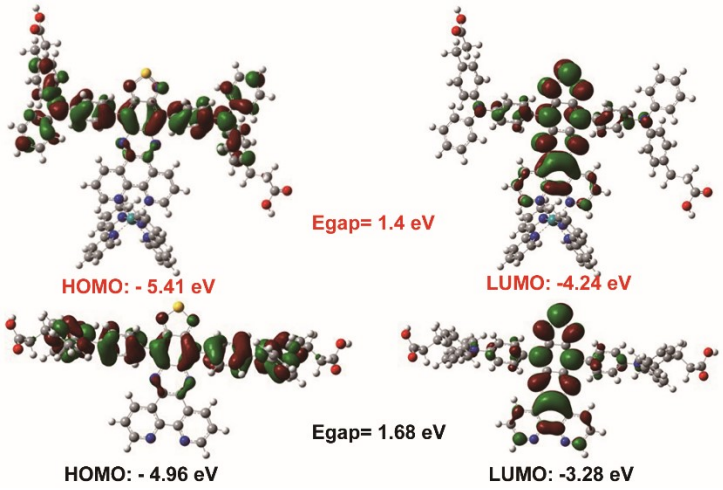

Figure S1. Calculated HOMO and LUMO of **H7** and **Ru-1** at the 6-31G(d) level. The HOMO and LUMO energy as well as Egap are presented.

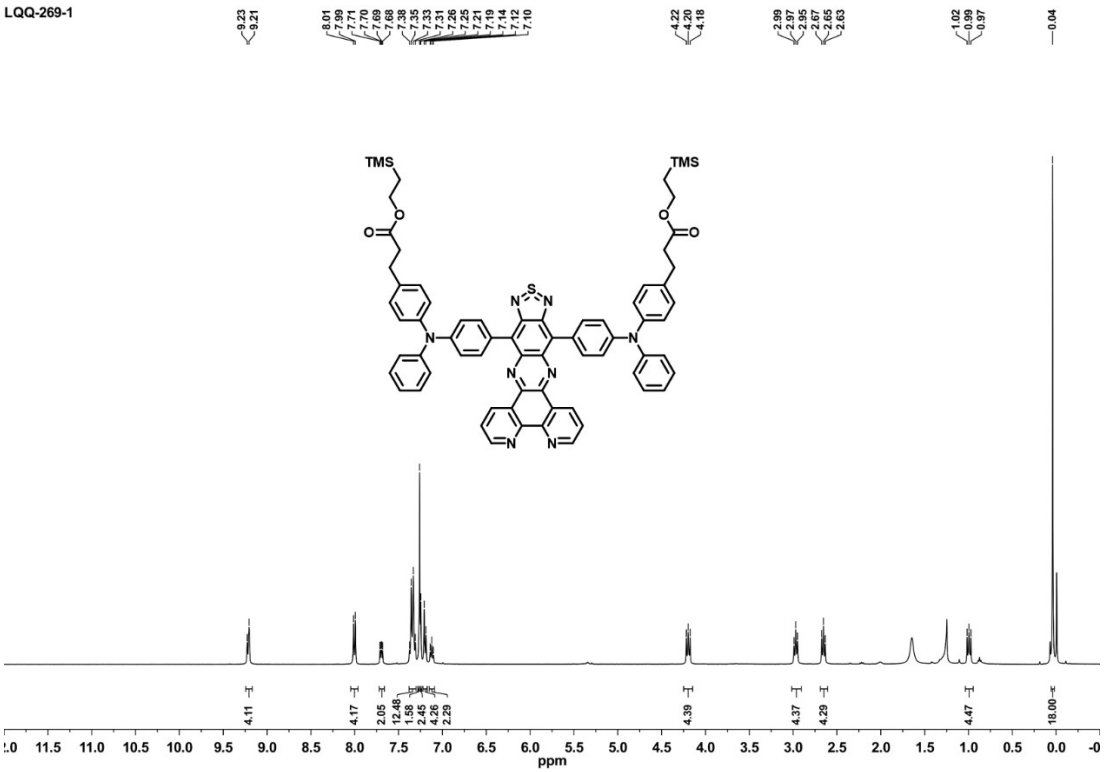

Figure S2. The ^{1}H NMR of **H7.**

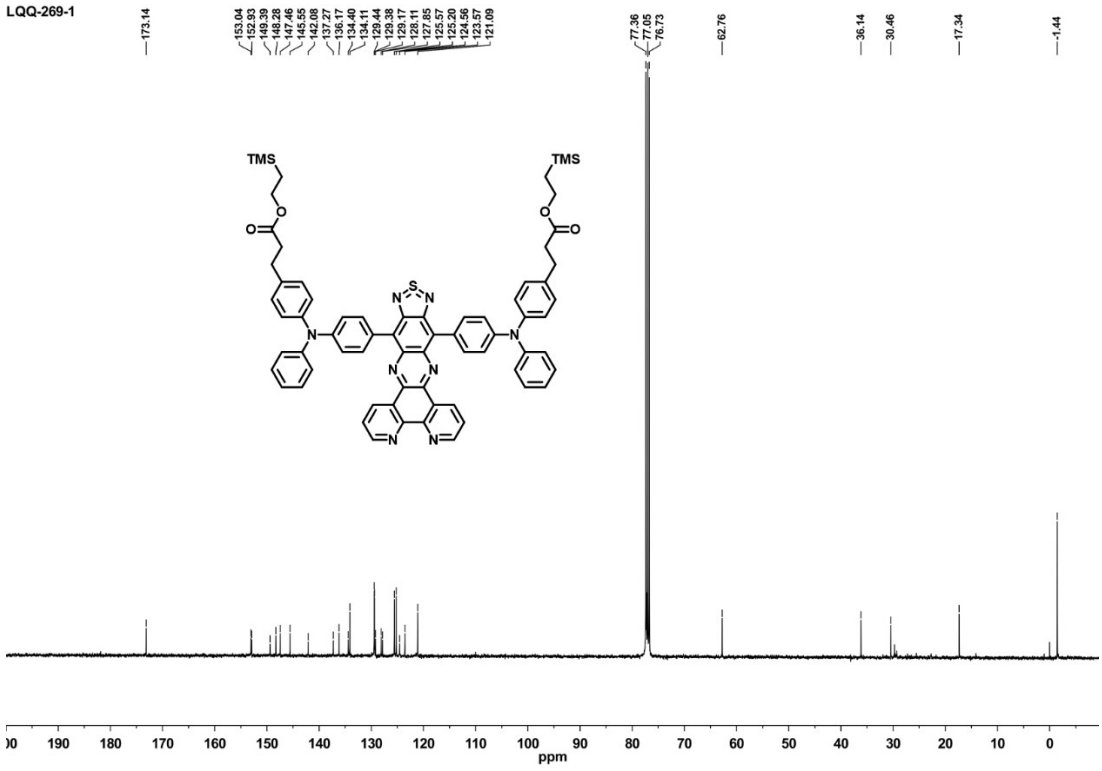

Figure S3. The ^{13}C NMR of **H7.**

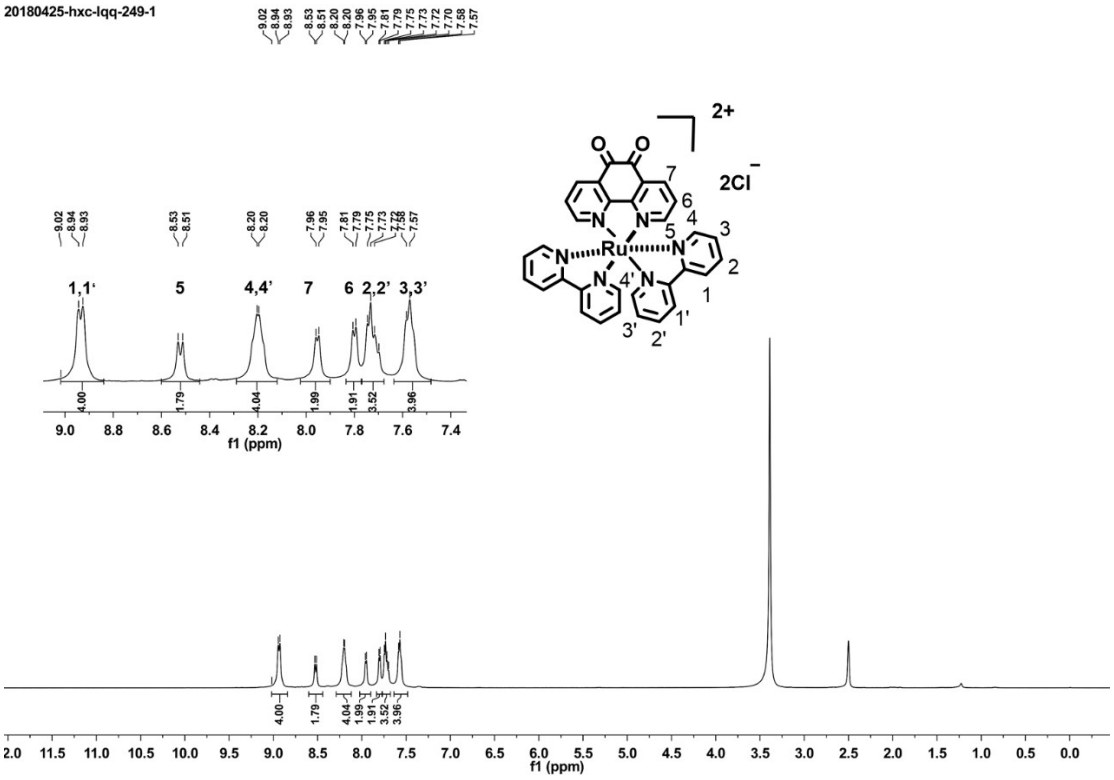

Figure S4. The ^{1}H NMR of **Ru(bpy)$_2$(phendione)Cl$_2$.**

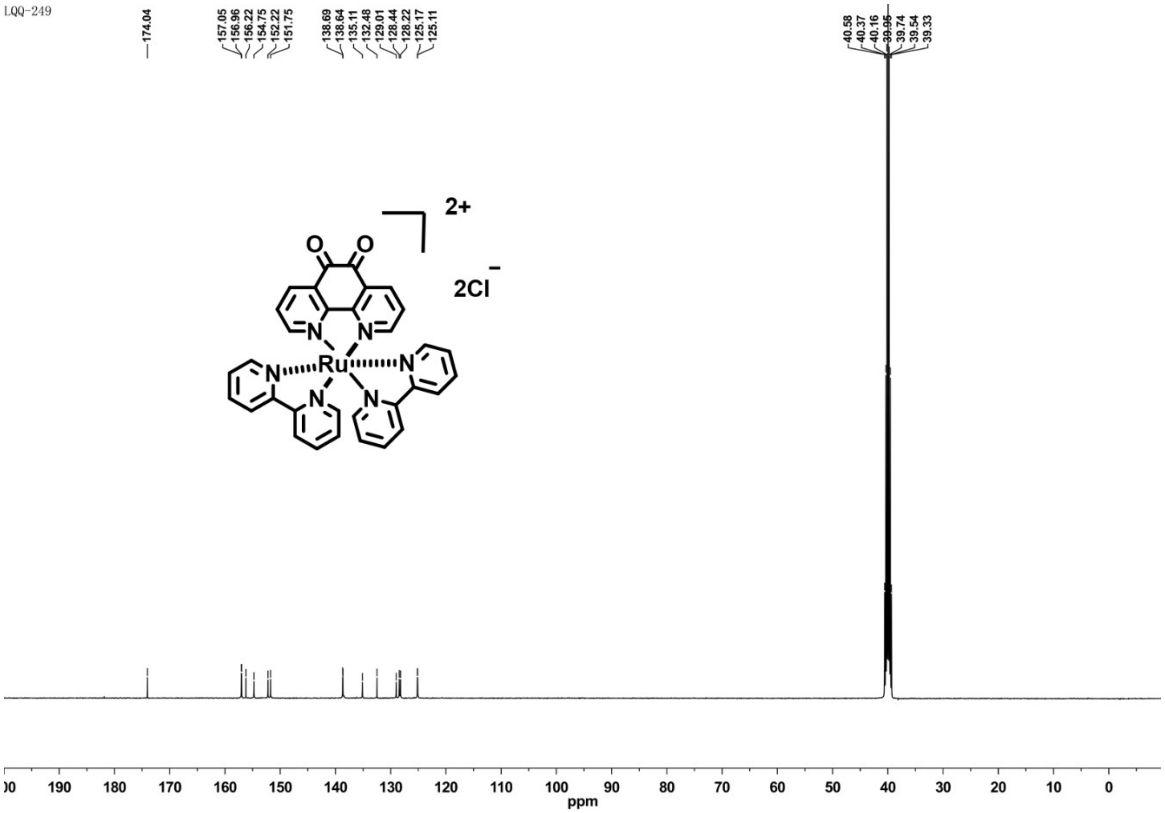

Figure S5. The ^{13}C NMR of **Ru(bpy)$_2$(phendione)Cl$_2$.**

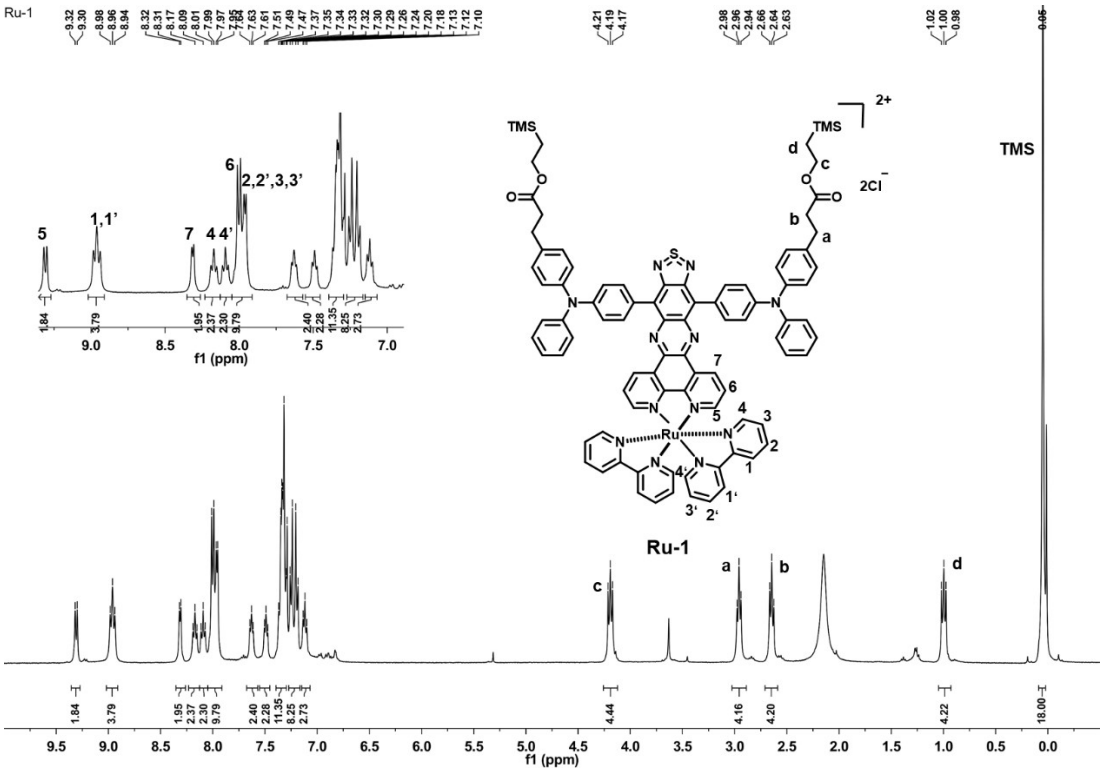

Figure S6. The ^{1}H NMR of **Ru-1.**

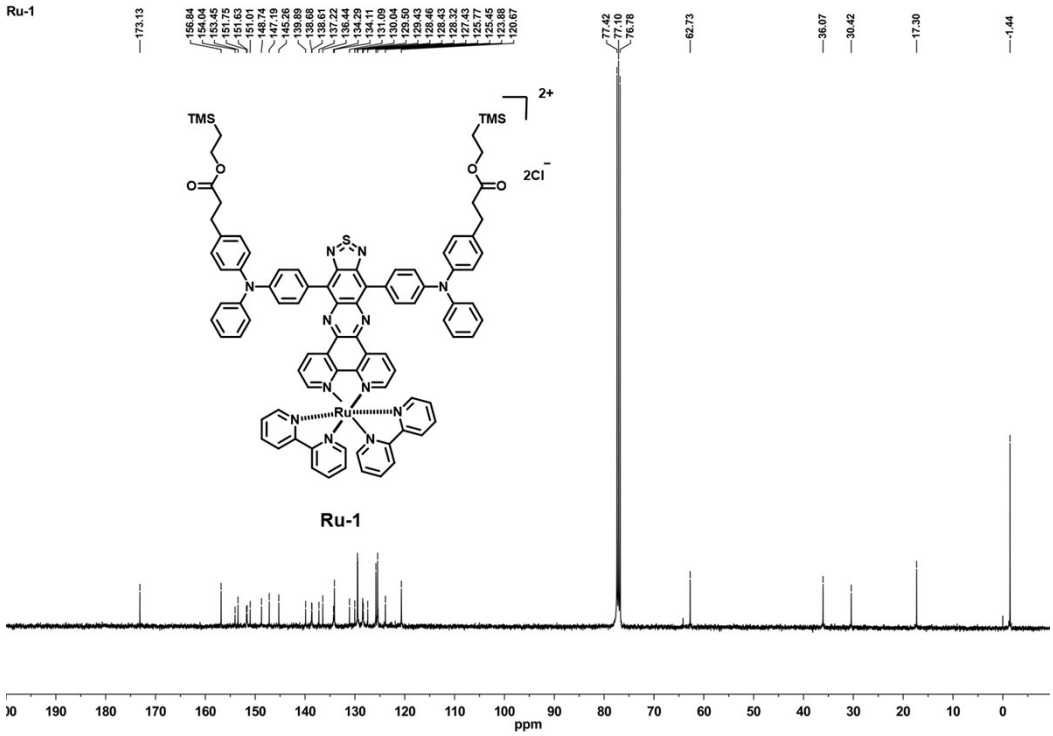

Figure S7. The ^{13}C NMR of **Ru-1.**

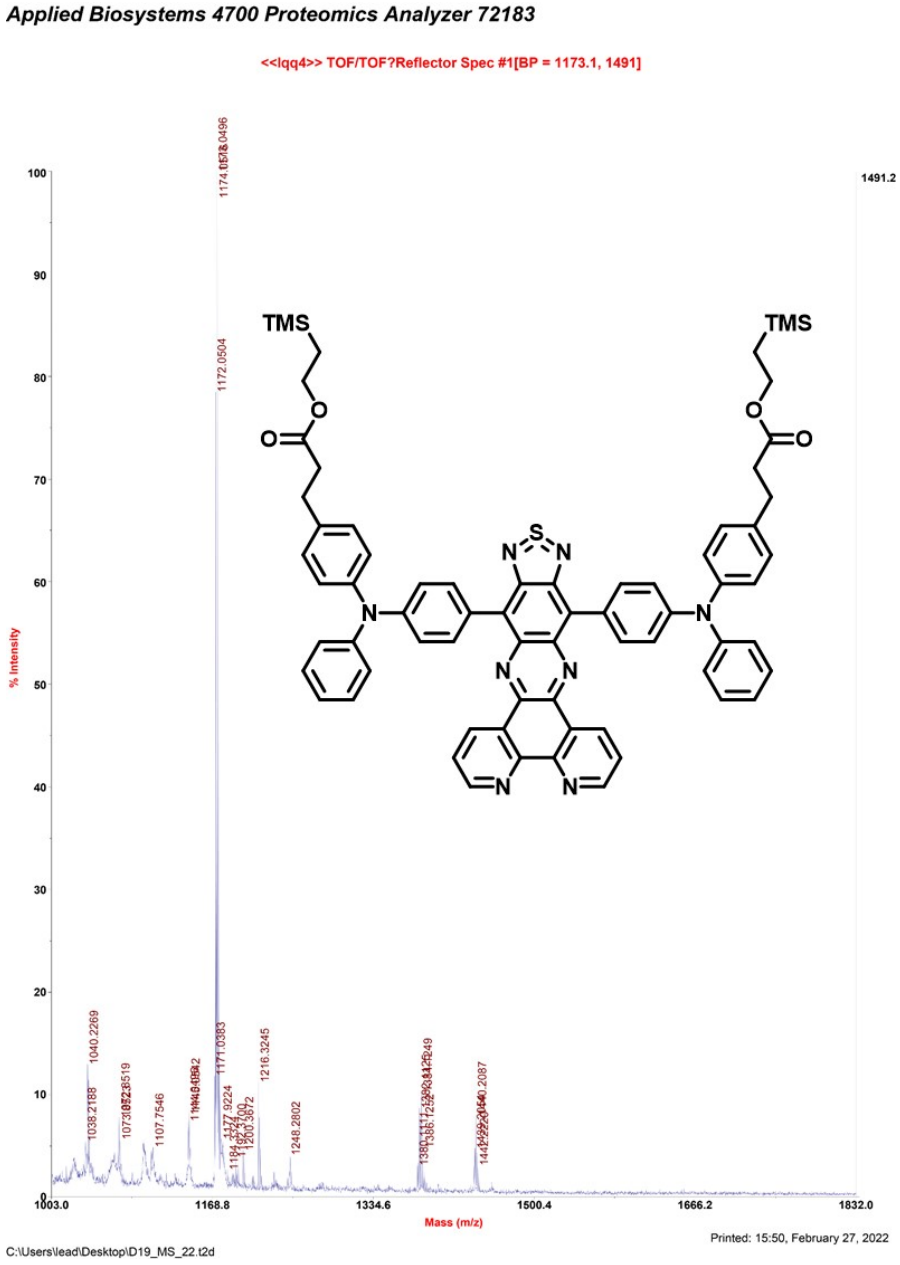

Figure S8. The MALDI-TOF of **H7.**

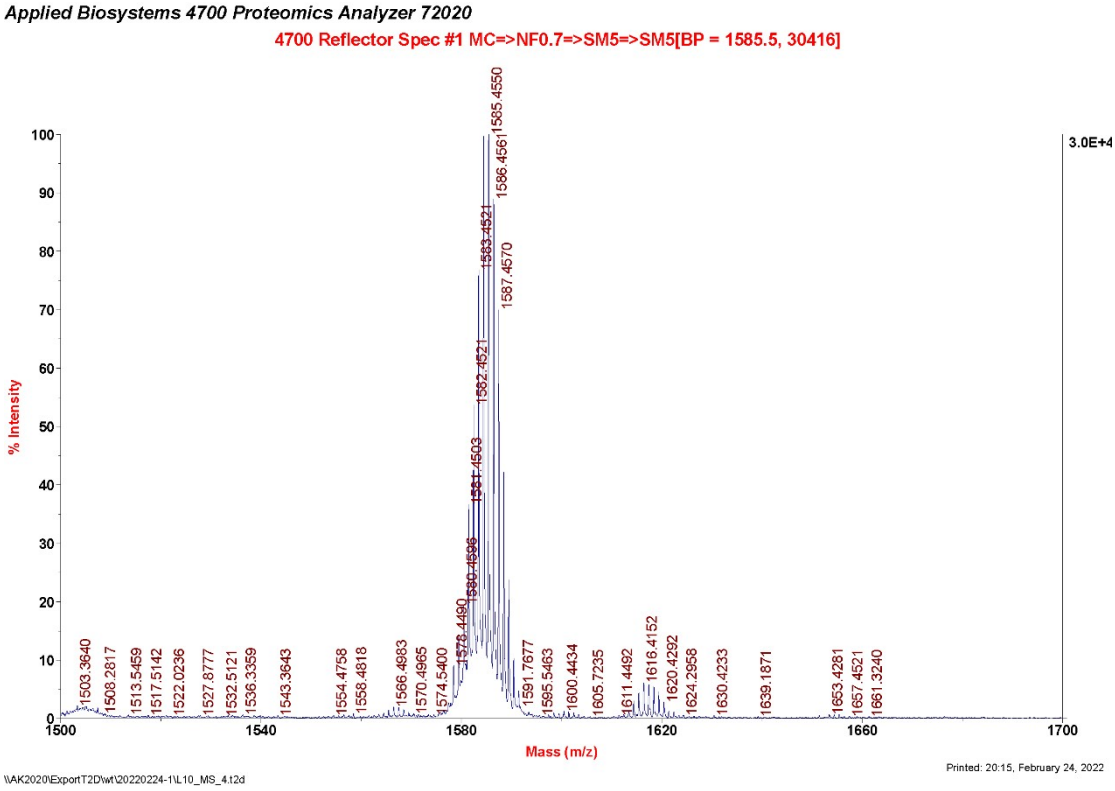

Figure S9. The MALDI-TOF of **Ru-1**.

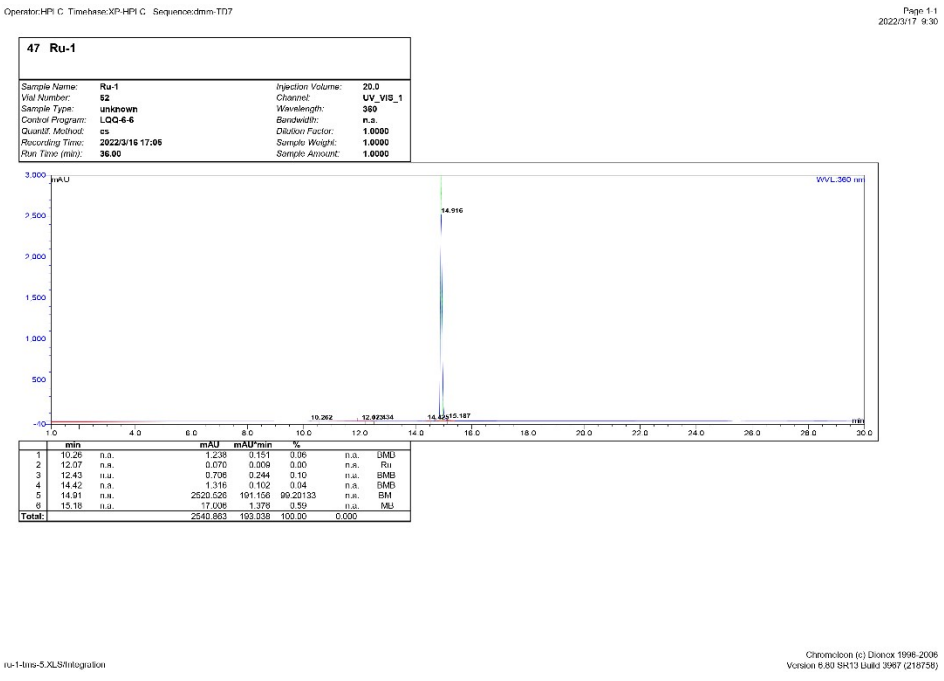

Figure S10. The HPLC of **Ru-1**.

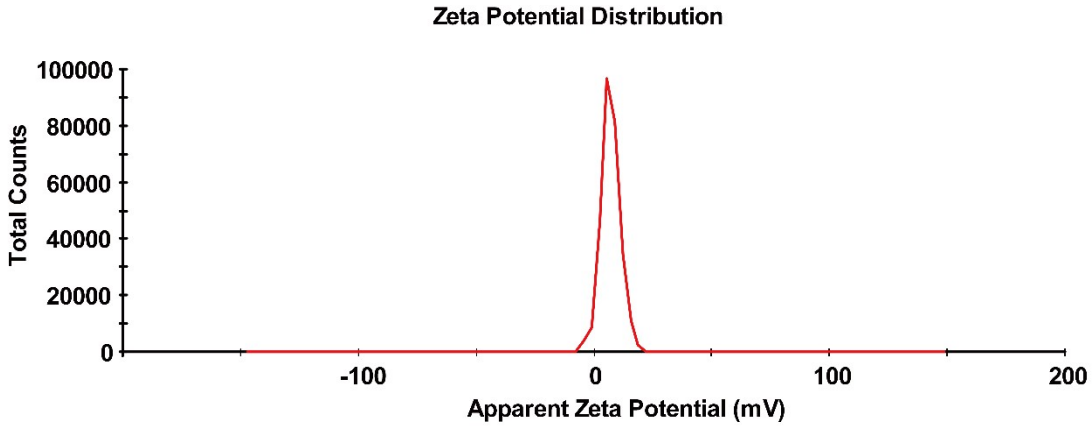

Figure S11. The Zeta potential of **Ru-1** dots.

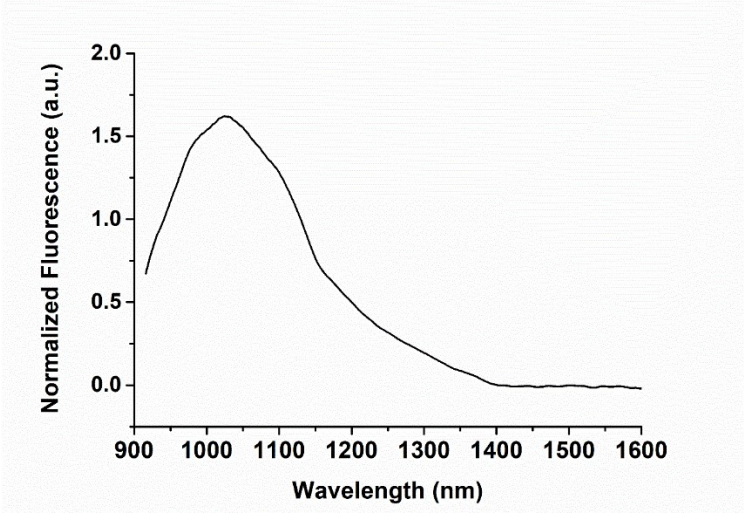

Figure S12. The fluorescence spectra of **Ru-1** dots in aqueous solution.

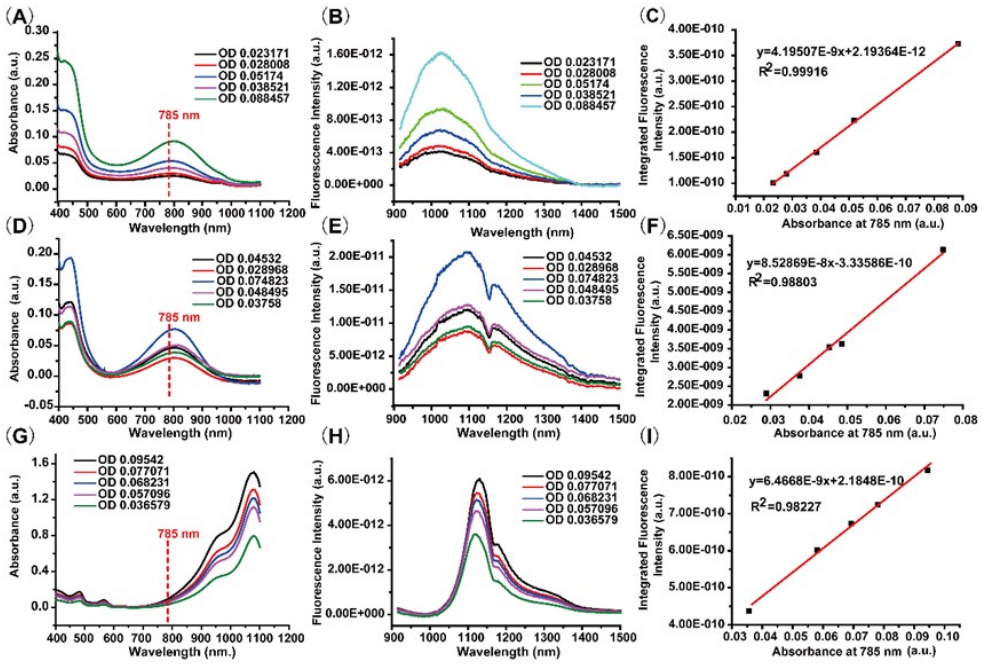

Figure S13. Absorbance (A, D, G) and fluorescence (B, E, H) spectra of **Ru-1** dots in water (A, B), **Ru-1** in DCM (D, E), and **IR-26** in DCE (G, H). The slope of **Ru-1 dots** in water (C), **Ru-1** in DCM (F), and **IR-26** in DCE (I). Fluorescence quantum yield measurements of **Ru-1** in DCM and **Ru-1** dots in water were calculated according to a standard equation in the previous literature [4]. The equation was below:

$$QY_{sam} = QY_{ref} \times \frac{S_{sam}}{S_{ref}} \times \left(\frac{n_{sam}}{n_{ref}}\right)^2$$

Where QY_{sam} is the QY of **Ru-1** dots, QY_{ref} is the quantum yield of IR-26 (~0.5%), S_{sam} and S_{ref} are the slopes obtained by linear fitting of the integrated fluorescence intensity of **Ru-1** dots (1000-1600 nm) and IR-26 (1000-1600 nm) against the absorbance at 785 nm. n_{sam} and n_{ref} are the refractive indices of their respective solvents (water:1.333 and DCM: 1.42).

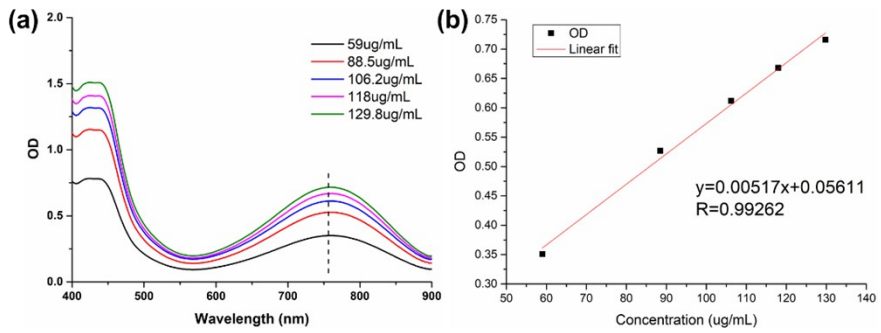

Figure S14. (a) the absorption spectra of **Ru-1** with different concentration in DCM. (b) the standard calibration curve plotted from the relationship between concentration and absorbance of

Ru-1.

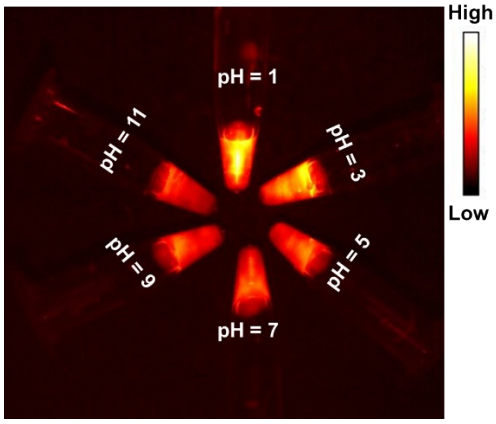

Figure S15. The NIR-II images of **Ru-1** dots at different pH values.

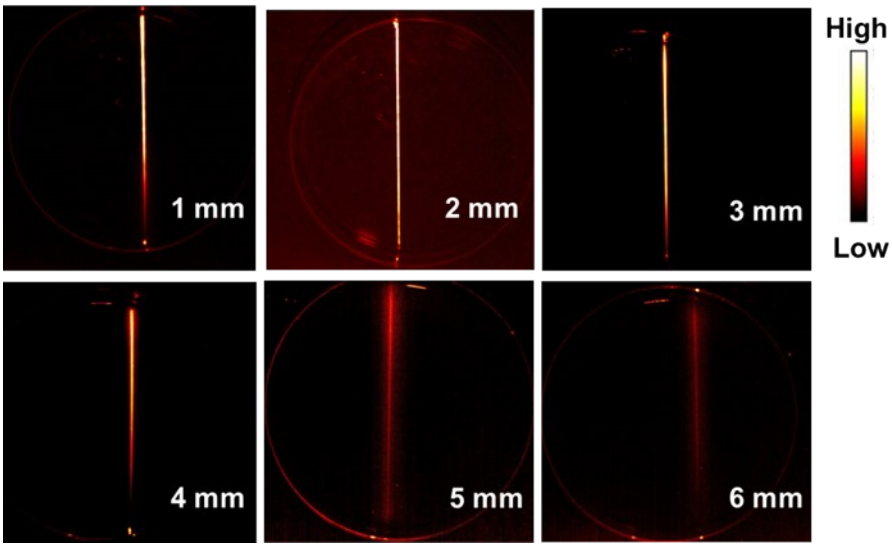

Figure S16. The NIR-II images of **Ru-1** dots immersed at various depths in 1% intralipid

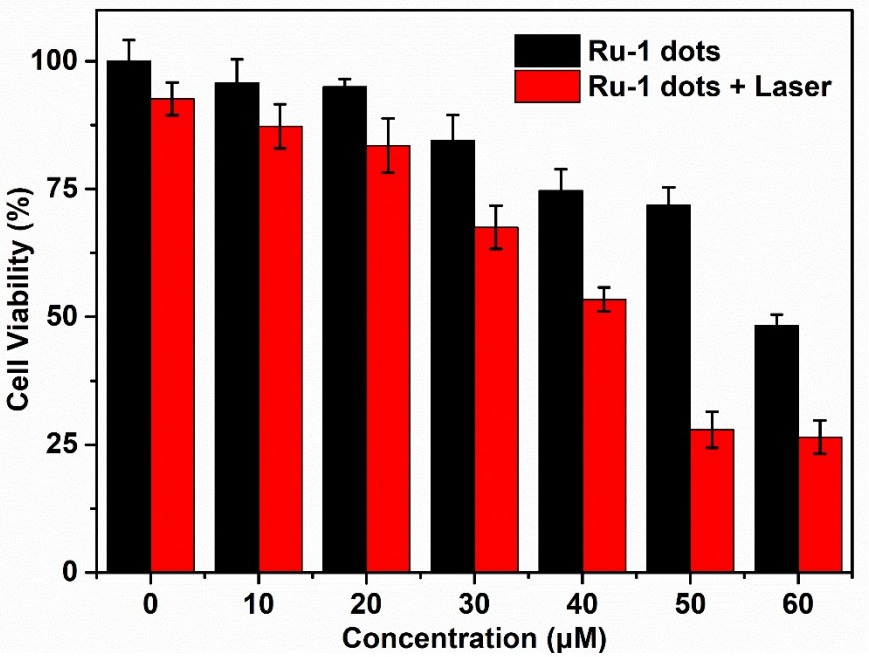

Figure S17. The cell viability of LO2 cell lines with **Ru-1** dots w/o laser irradiation (808 nm, 1 W cm-2) at different concentrations.

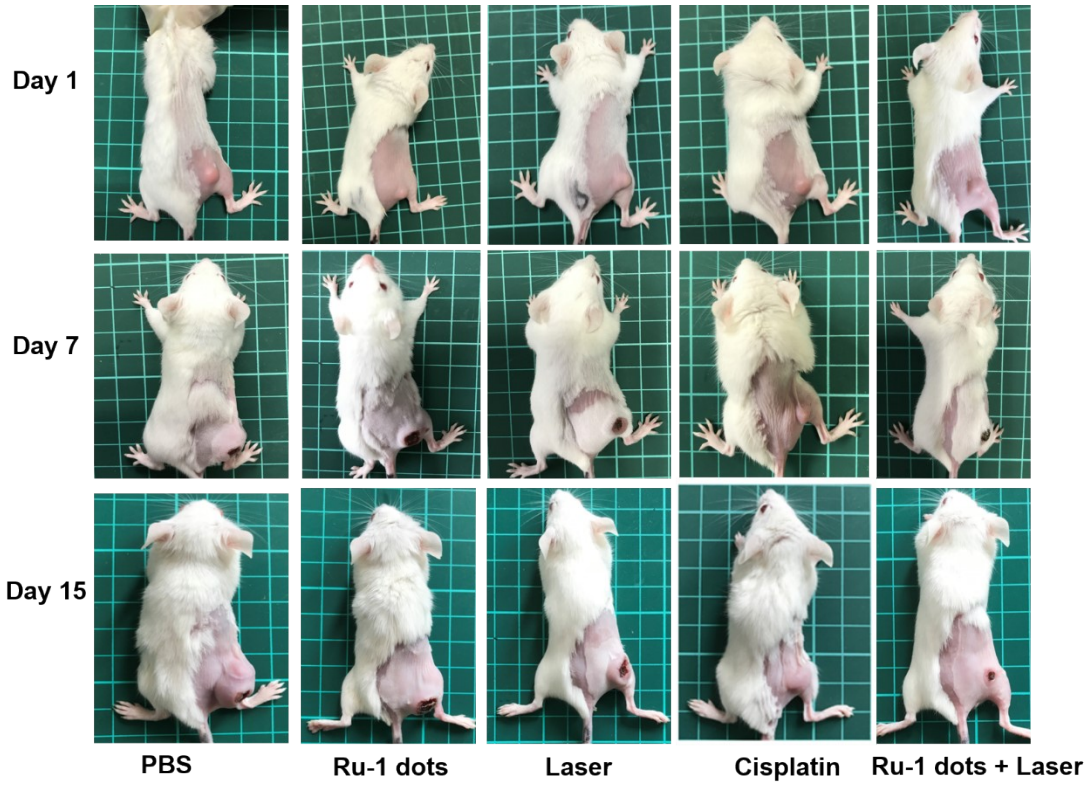

Figure S18. Representative digital photographs of tumor-bearing mice after different treatments.

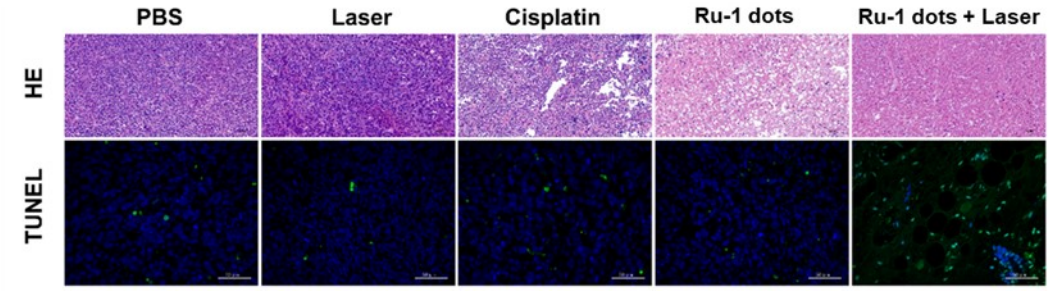

Figure S19 H&E and TUNEL stained histological images of tumor slices collected from different groups of mice after treatment for 24 h (Scale bar: 50 μm).

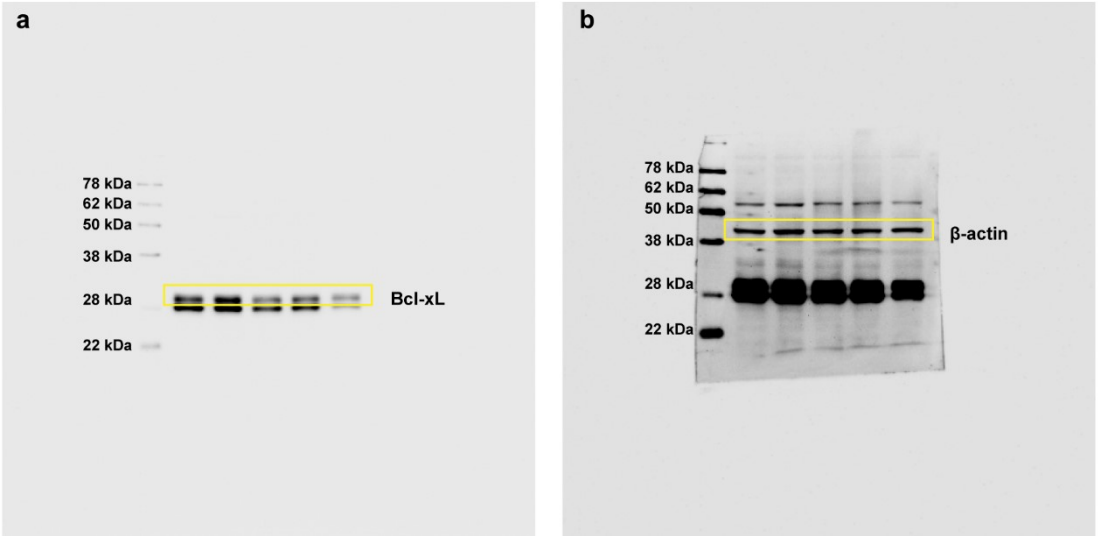

Figure S20 The complete uncropped western blot image of Bcl-xL (a) and the corresponding image of β-actin (b). (From left to right: Blank, Laser, Cisplatin, **Ru-1** dots, **Ru-1** dots + Laser)

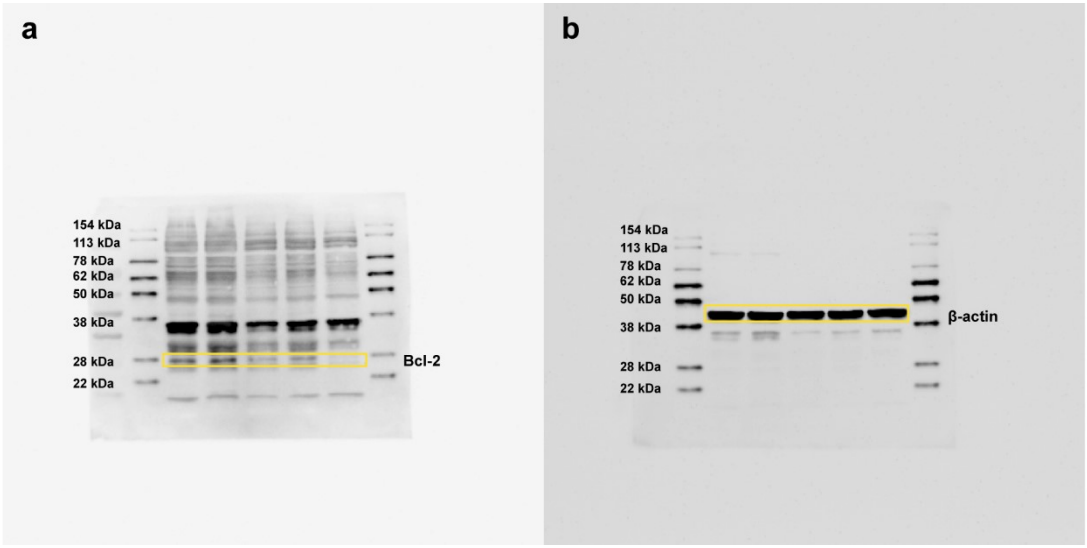

Figure S21 The complete uncropped western blot images of Bcl-2 (a) and the corresponding image

of β-actin (b). (from left to right: Blank, Laser, Cisplatin, **Ru-1** dots, **Ru-1** dots + Laser)

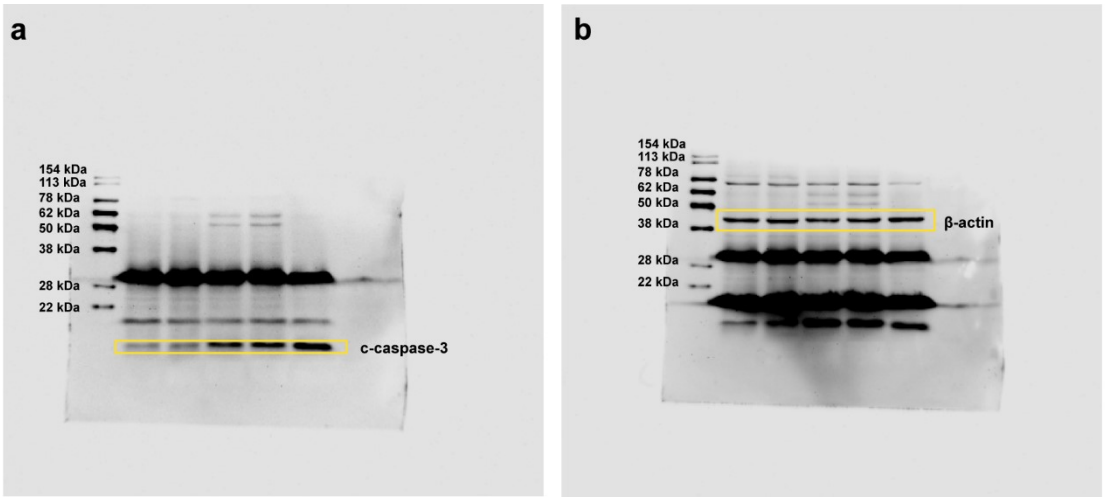

Figure S22 The complete uncropped western blot images of c-caspase-3 (a) and the corresponding image of β-actin (b). (from left to right: Blank, Laser, Cisplatin, **Ru-1** dots, **Ru-1** dots + Laser)

Reference

[1] Y. Liu, Q. Li, M. Gu, D. Lu, X. Xiong, Z. Zhang, Y. Pan, Y. Liao, Q. Ding, W. Gong, S. Chen, M. Guan, J. Wu, Z. Tian, H. Deng, L. Gu, X. Hong, and Y. Xiao, *J. Med. Chem.*, 2022, **65**, 2225–2237.

[2] Y. Zheng, Q. Li, J. Wu, Z. Luo, W. Zhou, A. Li, Y. Chen, T. Rouzi, T. Tian, H. Zhou, X. Zeng, Y. Li, X. Cheng, Y. Wei, Z. Deng, F. Zhou and X. Hong, *Chem. Sci.*, 2021, **12**, 1843-1850.

[3] X. Zeng, Z. Chen, L. Tang, H. Yang, N. Liu, H. Zhou, Y. Li, J. Wu, Z. Deng, Y.Yu, H. Deng, X. Hong and Y. Xiao, *Chem. Commun.*, 2019, **55**, 2541-2544.

[4] A. L. Antaris, H. Chen, K. Cheng, Y. Sun, G. Hong, C. Qu, S. Diao, Z. Deng, X. Hu, B. Zhang, X. Zhang, O. K. Yaghi, Z. R. Alamparambil, X. Hong, Z. Cheng and H. Dai, *Nat. Mater.,* 2016, **15**, 235-242.